SMART STRUCTURES IN THE ACTIVE CONTROL OF BLADE VORTEX INTERACTION

S.Hanagud, J.V.R. Prasad, T.Bowles and G.L.NageshBabu
School of Aerospace Engineering
Georgia Institute of Technology
Atlanta, Georgia, U.S.A. 30332-0150

Abstract

During the operation of a rotorcraft, rotor blades interact with vortices shed by preceding blades. As a result of the interaction, large pressure pulses are created at the leading edge of the airfoil. In this paper, feasibilities studies have been conducted to investigate if a combination of active camber changes by the use of smart structures concepts and optimum control techniques can be used to reduce the magnitude of the large pressure pulse created by the interaction of the airfoil and vortices shed by the preceding blade. The optimum control techniques used in this paper include a technique based on the use of a quadratic performance index and a technique based on H_∞ control concepts.

Introduction

During the past decade, there has been a considerable amount of research activity in the area of blade-vortex interaction (Ref 1-9). One of the important result of these studies is the characterization of a large pressure pulse near the leading edge of the airfoil. Some passive techniques(Ref 10-11) to reduce the magnitude of the pressure pulse have been studied. With the exception of Ref. 9 and 12, authors are not aware of any active control techniques to reduce the magnitude of the the vortex induced pressure pulse on the airfoil. In this paper, we would like to present results of a feasibility study to actively control the magnitude of the pressure pulse induced by the blade vortex interaction. In particular, we would like to consider a combination of the use of smart structures concept to actively change the shape of the airfoil and optimum control techniques. Two different optimum control techniques are considered in the present paper. The first method consists of the minimization of a quadratic performance index similar to that of Ref 12. A second method of optimum control uses results from recent developments in the area of H_∞ control theory(Ref. 13-17).

Smart Structures

During the past few years, there has been a considerable amount of research activity in the area of defining, analyzing and designing smart structures(Ref. 18-20). There are many definitions of smart structures. Some of the definitions proposed at a recent U.S. - Japan workshop on smart structures are as follows: An active material is defined as a material that is capable of functioning as a sensor and a actuator. An adaptive structure or an adaptive material is defined as a structure or a material that can respond to a stimulus. An example of adaptive material is the electro-rheological fluid. A smart structure is defined as a structure that contains embedded sensors, actuators, and processing units for detection, identification and control. These smart structures can react to different environments and provide the needed control. A smart material contains similar features of a smart structure at molecular levels. In a smart structure or a smart material, software can be embedded or used suitably to provide learning, memory or other types of (artificial) intelligence. Some times, the term " Intelligent materials and structures" are used when learning, memory and other artificial intelligence algorithms are incorporated.

In the present application, we would like to incorporate sensors, actuators and controllers to produce a desired change in the shape of the airfoil to reduce the magnitude of the (shed) vortex induced pressure pulses. In this context, we are concerned with a smart structure. At Georgia Tech, we have demonstrated the use of shape memory alloys and piezoelectric transducers to effect selected shape changes of the airfoil. The dynamics of the shape changes induced by the shape memory alloys can be approximated by using appropriate mathematical models. First we have used this concept and mathematical models to theoretically study the feasibility of controling the blade-vortex interaction effects. In this phase of study, a constant gain controller has been designed by minimizing a selected performance index that will assume a reduction of the peak pressure with minimal control forces. As a next step, we have used H_∞ control concepts to accommodate rapid shape changes that can be accomplished by the use of piezoceramic transducers.

Problem Setting

In this paper, we are primarily concerned with the feasibility studies. The interaction of an airfoil and a vortex is modeled by considering two dimensional,

unsteady, inviscid, incompressible subsonic flow equations. The needed interactions have been calculated by using a computational fluid mechanics code (CFD) based on panel methods. The panel method used is a standard panel method that is based on the concept of the conservation of vorticity at each time step, the association of a vortex sheet with uniform vorticity for each element or panel of the airfoil and the calculation of the associated sensitivity coefficients and the stream function of the airfoil(Ref.21).

In order to model the needed changes in the shape of the airfoil, it is assumed that shape changes are induced by rotating different panels by different amounts from their initial positions by the use of smart actuators like shape memory alloys or piezoceramic transducers. It is assumed that a continuity of the shape of the airfoil is maintained.

Resulting panel equations to be solved for the determination of the coefficient of the j^{th} panel are as follows.

$$\psi_a + \sum_{j=1}^{N} A_{ij}\gamma_j = u_\infty y_i - v_\infty x_i + \sum_{k=1}^{M} W_{ik}\gamma_k + \psi_v + \psi_{sa} \quad (1)$$

where

ψ_a = stream function of the airfoil
A_{ij} = sensitivity coefficient of the vortex sheet at panel j due to the stream function at point i
γ_j = distributed vorticity on panel j
u_∞ = x component of the free stream velocity
v_∞ = y component of the free stream velocity
x_i = x co-ordinate of the point i
y_i = y co-ordinate of the point i
w_{ik} = Sensitivity coefficient of the vorticity in the wake on the stream function on the k^{th} panel with a vorticity of γ_k in the wake at control point i on the airfoil
ψ_v =contribution to the stream function due to the concentrated vorticity of strength Γ at a distance r from the control point i
M =no of time steps
N =no of panels
ψ_{sa} =contribution due to smart actuation to the stream function

The quantity ψ_v for a concentated vorticity of strength Γ is given by(Ref.21)

$$\psi_v = \frac{-\Gamma}{2\pi} ln(r) \quad (2)$$

Where r is the distance from the vortex to the point of consideration in the flow field.

Contributions due to smart actuators ψ_{sa} can be calculated as follows. The velocity component in the y- direction is assumed to be equal to the sum of the free stream velocity and the additional contribution because of panel rotation due to smart actuation. This additional contribution caused by the panel rotation will vary depending on whether this rotation is due to a left side hinge or right side hinge. If $w_k, \dot{w}_k$ represent the angular rotation and angular velocity for the k^{th} hinge, for a left side hinge at x_h, this contribution can be written as

$$\psi_{sa} = \frac{-\dot{\omega}_k}{2}(x - x_h)^2 - u_\infty \omega_k (x - x_h) \quad x > x_h \quad (3)$$

For a right hinge at x_p, this contribution can be written as

$$\psi_{sa} = \frac{-\dot{\omega}_p}{2}(x - x_{p-1})^2 - u_\infty \omega_p (x - x_{p-1}) \quad x_{p-1} < x > x_p \quad (4)$$

where x_{p-1} represents the x coordinate of the p-1^{th} hinge from the leading edge. Then the total contribution due to s_r right side hinges and s_l left side hinges can be written as

$$\psi_{sa} = \sum_{p=1}^{s_r} \frac{-\dot{\omega}_p}{2}(x - x_{p-1})^2 - u_\infty \omega_p (x - x_{p-1}) \quad x_{p-1} < x < x_p + \sum_{k=1}^{s_l} \frac{-\dot{\omega}_k}{2}(x - x_h)^2 - u_\infty \omega_k (x - x_h) \quad x > x_h \quad (5)$$

When the flow is unsteady, some vortices are shed into the wake. These vortices also influence the vorticity on the airfoil. At each time step, a panel of length l and vorticity $\gamma_u + \gamma_l$ is added to the down stream of the trailing edge. Here l is the length of the panel at the trailing edge and γ_u, γ_l are the vorticities at the upper and lower surface panels at the trailing edge. Also panels that are already in the wake move downstream. In order to account for this, the equation (1) is supplemented by the conservation of vorticity equation given by

$$\sum_{j=1}^{n} \gamma_j l_j + \sum_{k=1}^{M} \gamma_k l_k = 0 \quad (6)$$

to determine the unknown γ_j and ψ_a. Here l_j and l_k are lengths of the panel on the airfoil and in the wake respectively.

The coefficient of pressure C_p^j for the j^{th} panel is, given by

$$C_p^j = \sqrt{1 - \frac{\gamma_j^2}{v_\infty^2}} \quad (7)$$

Optimum Control Based on a Quadratic Performance Index

The dynamics of the camber changes, due to the rotation of panels, is assumed to be

$$\dot{\omega}_k = R\omega_k + K_p(C_p - C_{pss}) \quad k = 1, 2, ..s \qquad (8)$$

where K_p is the gain to be computed for the s^{th} actuator. Here C_{pss} represents the steady state coefficient of pressure. The quantity R depends on the smart actuator dynamics. Then the performance index to be minimized is chosen as

$$J = \int_0^{t_f} \{a(C_p - C_{pss})^2 + \sum_{k=1}^{s} b_k \omega_k^2\} dt \qquad (9)$$

In this equation, a and b_k are the weighting factors and t_f represent the total duration for which the performance index is evaluated.

Optimization Procedure

For minimizing the performance index J chosen, method of steepest descent is used(Ref 22). This is an iterative method where the total time t_f is discretized in to M time steps. The performance index and panel rotation dynamics in the discretized form can be written as

$$J = \sum_{i=0}^{M} \{a(C_{pi} - C_{pss})^2 + \sum_{k=1}^{s} b_k \omega_{ki}^2\} \qquad (10)$$

$$\dot{\omega}_k^{i+1} = R\omega_k^i + K_p(C_p^i - C_{pss}) \qquad (11)$$

The iteration starts with an initial guess for the gain K_p. Using zero initial conditions for ω_k and $\dot{\omega}_k$ initial value of C_p is computed from the equations 1-7. This value of C_p is used to determine the performance index J^0, the performance index at time zero and ω_k^1 and $\dot{\omega}_k^1$ at time Δt. Here Δt denote the discretized time step. Thus, using ω_k^i and $\dot{\omega}_k^i$, value of C_{pi} and hence J^i are computed at the i^{th} time step. Using the value of C_{pi}, the values of ω_k^{i+1} and $\dot{\omega}_k^{i+1}$ at i+i^{th} time step are computed. This process is continued for a total M steps to obtain the total performance index and it completes one iteration.

In order to move the total performance index towards minimum, the gain K_P is modified as

$$K_p = K_p - \tau \frac{\partial J}{\partial K_p} \qquad (12)$$

and another iteration for the computation of J is repeated. Here τ is a positive number chosen such a way that J always reduces with each iteration. This iterative process of updating the K_p is continued till the value of $\frac{\partial J}{\partial K_p}$ converges to zero and the value of K_p at which $\frac{\partial J}{\partial K_p}$ approaches zero is the optimum gain.

Results With a Quadratic Performance Index

In order to compare with Ref.12, where only one flap motion was considered, here camber is assumed to be changed by rotations at a point near the leading edge and at another point near the trailing edge. The resulting camber change is as illustrated in figure 1.

The hinge location near the leading edge is chosen to be 0.05 ft from the leading edge. The hinge location for the trailing edge is at 1.125 ft from the leading edge. A proportional controller is designed based on the minimization of the performance index given in equation 9. For an angle of attack of 10^o, the value of K_p has been obtained as 7.88. Assumption here is that the rotation angles due to smart actuation at the leading and trailing edge are same. A limit on the maximum rotation is set at 10 ^{o}. A staring vortex of strength($\frac{\Gamma}{v_\infty c}$) 0.2 at a location of half the chord distance below and 4 chords distance ahead of the leading edge is assumed. A plot of C_p for the controlled and uncontrolled cases is shown in Figure 2. In this figure t is time in sec. and c is the chord length. Angular rotation and velocity with respect to the non dimensional time are shown Figure 3 and Figure 4. From the plots it can be observed that a reduction of almost 80 percent of the peak pressure can be obtained by the rotation of panels there by changing the shape of the airfoil.

H_∞ Controller

Using a quadratic performance index criterion, the average value of the difference between the unsteady pressure pulse and steady state pressure pulse has been minimized. However, using this process involves computation of C_p value at each iteration which is not computationally efficient. As the effect of the blade-vortex interaction is a large pulse at the leading edge, it is decided to explore a H_∞ controller that reduces the peak of the difference of unsteady pressure pulse to the steady state pressure pulse. If C_p-C_{pss} is denoted as the error, it is the objective of this controller to reduce the error to a minimum. Variation of this error with time is shown in Figure 5. An ordinary differential equation has been constructed to approximately represent this variation of error with time. This equation is constructed in such a way that its solution encloses most of the error at all times. A constructed curve enclosing the error is shown in Figure 6. The equation constructed is a first order ordinary differential equation with an impulse forcing function given by

$$\dot{x} = Ax + b_1 f \qquad (13)$$

This equation is the open loop equation for the plant for which the controller is designed. The objective here is to reduce the state x of the plant to minimum. Here x represents C_p-C_{pss}.

Control action is assumed to be provided through camber changes resulting from smart actuation. Again, the motion of both the leading and trailing edge are assumed to be equal. It is assumed that C_p varies linearly with the panel motion. The closed loop

equation for the error x is given by

$$\dot{x} = Ax + b_1 f + b_2 \omega_k \quad (14)$$

Now the objective is to choose suitable ω_k that minimizes the maximum value of x for a given disturbance f which is a function of the vortex Γ. This can be stated as that of minimizing the supremum of x/f. This results in minimizing the infinity norm of the transfer function between x and f.

Control Procedure

Minimizing the two norm of x/f is also known as H_∞ control with state feedback. In the form of a block diagram of transfer functions, we can write the control system as shown in Figure 7. As the output is x it self, e and y in the block diagram 7 are equal to x it self.

Here P is the transfer function model of the airfoil, f is the disturbance and e is the error to be minimized. The controller K is to be designed to meet this objective of minimizing e for f encountered in the operation.

In frequency domain, we can write the control equations as

$$\begin{Bmatrix} e \\ y \end{Bmatrix} = \begin{bmatrix} P_{11} & P_{12} \\ P_{21} & P_{22} \end{bmatrix} \begin{Bmatrix} f \\ u \end{Bmatrix} \quad (15)$$

Then

$$e = f_l(P, K) f \quad (16)$$

where

$$f_l(P, K) = [P_{11} + P_{12} K (I - P_{22} K)^{-1} P_{21}]$$

In fact, we will be minimizing $f_l(P, K)$ with a weight W to account for the input disturbance. This minimization will be accomplished by using the Glover-Doyle algorithm [14]. In this procedure, $f_l(P, K)$ is first transformed to $f_l(T, Q)$.

$$\begin{aligned} T_{11} &= P_{11} - P_{12} U_o \hat{M} P_{21} \\ T_{12} &= -P_{12} M \\ T_{21} &= \hat{M} P_{21} \\ T_{22} &= 0 \end{aligned} \quad (17)$$

In this equation, Q is to be determined and quantities M and $\hat{M}$are introduced following Bezout's theorem such that

$$\begin{aligned} P &= NM^{-1} = \hat{M}^{-1} \hat{N} \\ M &= [F(SI - A - BF)^{-1} B + I] \\ N &= [(C + DF)(SI - A - BF)^{-1} B + D] \\ \hat{M} &= -[C(SI - A - HC)^{-1} H + I] \\ \hat{N} &= [C(SI - A - HC)^{-1} (B + HD) + D] \end{aligned} \quad (18)$$

where F and H are such that $A+BF$ is asymptotically stable (state feedback problem) and $A+HC$ is stable (observer problem). A,B,C,D are the realization of the plant P. Similarly U_o can be defined using fractional representation of any stabilizing controller K_o.

Then the Glover Doyle algorithm consists of first finding vectors x_∞ and y_∞ that are the solutions to the associated Ricatti equations. Then, using these vectors, a stabilizing controller can be calculated. then an iterative procedure is used to find minimum of the norm of e/f by varying Q

Results With a H_∞ Controller

The constants A,b_1,f constructed for the ordinary differential equation are -1.556, 13.51 and δ(t-3). Here δ denotes the Dirac Delta function. Based on the algorithm due to Ref 14, a H_∞ controller has been designed. Time domain equation of the controller designed is given by

$$\dot{\omega}_k(t) = -1.07e^7 \omega_k + 474366.8(C_p - C_{pss}) \quad (19)$$

and frequncy domain representation is given by

$$\omega(s) = \frac{474366.8(C_p - C_{pss})}{s + 1.07e^7} \quad (20)$$

. Bode plot representation of this controller has been shown in Figure 8. Solving equation 19, rotation angle of the panel,ω_k can be obtained as

$$\omega_k(t) = 0.047(1 - e^{-1.07e^7 t})(C_p - C_{pss}) \quad (21)$$

To evaluate the effectiveness of the controller thus designed, it has been incorporated in the computation of C_p. The coefficient of pressure obtained using H_∞ controller is shown in Figure 9. Panel rotation angle variation with time has been shown in Figure 10. From the Figures 3 and 10, it can be seen that, using H_∞ controller, the panel rotation angle required for the reduction of vortex interaction on pressure pulse is always less than 5°, where as the panel rotation angle for the controller designed on quadratic performance criteria reaches a value of 10° for almost the same reduction of the pressure pulse.

In effect at any instant of time, the panel rotation (equation 21) is proportional to the difference of the C_p and C_{pss}. This proportionality is due to the approximation of the control system by a simple ordinary differential equation (equation 14). A more accurate approximation may result in a more effective dynamic compensator rather than a proportional controller. However, it is to be noted that the gain in this case (H_∞) is less than the gain when a quadratic performance index was used and consequently pressure reduction is also less. But the optimization process involved to obtain this gain does not involve repeated computation of panel code. A very simple approximation (equation 14) was used to avoid this repeated use of panel code. A better or modified models for the approximation of the error may result in a more effective controller with minimal control values of ω_k.

Conclusions

Feasibility study to reduce the blade vortex interaction is presented. Concepts of smart structures and

optimum control theory are used. A proportional controller that minimizes a quadratic performance index and a H_∞ controller that minimizes the peak magnitude of the error are designed. Simple first order ordinary differential equation used here to represent the error should be modified to reflect the more complicated phenomena of blade-vortex interaction. Before proceeding from the feasibility to practical designs, we need to consider three dimensional panel codes and need to evaluate all possible adverse effects similar to those pointed by Ref 9. MIMO controllers and aeroelastic effects should be considered.

Acknowledgements

The authors gratefully acknowledge support for this work from U.S Army research Contract DAAL03 - 88-c-0003, to create CERWAT, Center for Excellency in Rotory Wing Aircraft Technology.

References

1. Caradonna,F.X., Strawn,R.C. and Bridgeman, J.O., An experimental and computational study of rotor-vortex interactions,**Vertica**, Vol.12, No 4, 1988.

2. Strauss,J., Renzoni,P., and Mayle,R.E., Airfoil pressure measurements during a blade vortex interaction and a comparison with theory, **AIAA, 26 th Aerospace Science Meeting**, Paper no 88-0669,Jan. 1988.

3. Kokkalis,A. and Galbraith,R.A.McD.. Results from the glasgow university BVI facility, **13 th European Rotor Craft Forum**, Sept. 1987.

4. Caradonna,F.X., Lautenschlager,J. and Silva,M., An experimental study of rotor-vortex interactions,**AIAA, 26th Aerospace Science Meeting**, Paper no 88-0045,Jan. 1988.

5. Tang,W. and Sankar,L.N., Strong blade vortex interactions including collision, **ASME, Fluid Engineering Divison**, Vol. 52, 1987.

6. Hsu,A.T. and Wu,J.C., Vortex flow model for the blade-vortex interaction problem, **AIAA Journal** Vol. 26, May. 1988.

7. Srinivasan, G.R., McCroskey,W.J. and Baeder,J.D., Aerodynamics of two dimensional blade-vortex interaction, **AIAA Journal** Paper no. 85-1560.,July 1985.

8. Hardin,J.C. and Lamkin,S.L., Concepts for reduction of blade vortex interaction noise, **Journal of Aircraft**, Vol. 24, Feb. 1987.

9. Brooks,T.F., Booth,Jr., E.R., Jolly,Jr.. J.R., Yeager,Jr., W.T. and Wilbur,M.L.. Reduction of blade-vortex interaction noise through higher harmonic pitch control **American Helicopter Society**.Jan. 1990.

10. Boxwell, D.A., Schmitz, F.H.. Splettstoesser, W.R., Helicopter model rotor blade-vortex interaction impulsive noise: Scalability and parametric variations, **Journal of the American Helicopter Society**, Vol. 32, Jan. 1987.

11. Mueller,M., Influence of winglets on rotor aerodynamics, **Proceedings of the 43 rd Annual Forum of the American Helicopter Society**,1987.

12. Prasad,J.V.R, Bowles,T. and Vandekerckhove,D., Active control of blade vortex interaction, bf Proceedings of the A.H.S. International Technical Specialists Meeting on Rotor Craft Basic Research,Paper no 52, March. 1991.

13. Doyle,J.C., Robustness of multiloop linear feedback systems, **Proc. 17th IEEE Conference Decision and Control (CDC)**, 1978.

14. Doyle, J.C., Glover, K., Khargonekar, P.P, and Francis,B.A., State space solutions to standard H_2 and H_∞ control problems, **American Control Conference**, 1988. 1988.

15. Glover,K. and Doyle,J.C., State-space formulae for all stabilizing controllers that satisfy an H-infinity norm bound and relations to risk sensitivity, **Systems and Control Letters** Vol. 11, 1988.

16. Maciejowski,J.W., Multivariable feedback design, **Addision - Wesley Publishing Company**, 1989.

17. Francis,B.A., A course in H_∞ control theory, **Springer - Verlag**, 1987.

18. Rogers, C.A., Barker, D.K., and Jaeger, C.A., Introduction of smart structures and materials", **Smart Materials ,Structures and Mathematical Issues**, Ed by C.A. Rogers, Technomic Publishing Co. 1988.

19. Hanagud,S., Obal,M.W. and Calise, A., Piezoceramic devices and PVDF Films as smart sensors and actuators for intelligent structures", **Smart Materials, Structures and Mathematical Issues**, Ed by C.A. Rogers, Technomic Publishing Co., 1988.

20. Hanagud,S., Glass,B.J. and Calise, A.J., Piezoceramics and artificial intelligence concepts in time varying smart structures, **Proc. SPIE conference on fiber optic smart structures and skins**, 1989.

21. Smetana, F.O. et. al., Light aircraft lift, drag and moment prediction: A review and analysis, **NASA CR 2523** May 1975.

22. Bryson,A.E. and Ho, Y.C., Applied optimal control , **Hemisphere Publishing Corporation**, 1975.

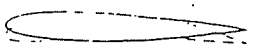

igure 1. Camber changes for the reduction of blade-vortex interaction

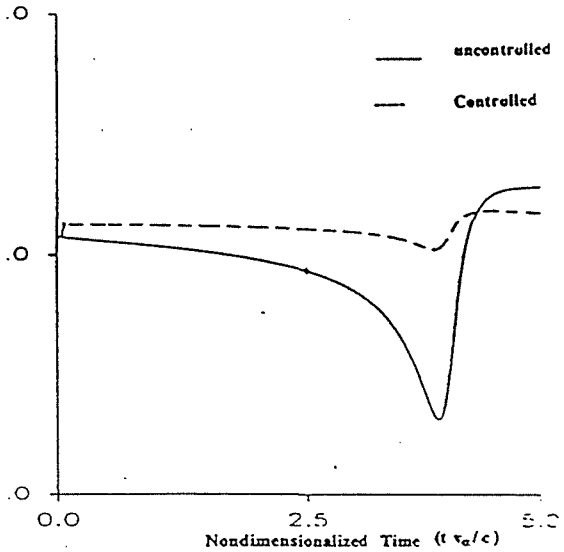

Figure 2. Variation of coefficient of pressure using a controller designed based on quadratic performance index

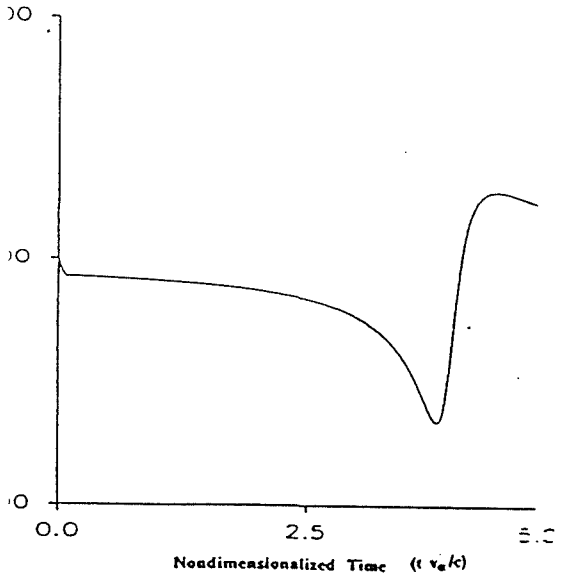

Figure 3. Panel angular rotations at the leading and trailing edges using the controller designed based on quadratic performance index

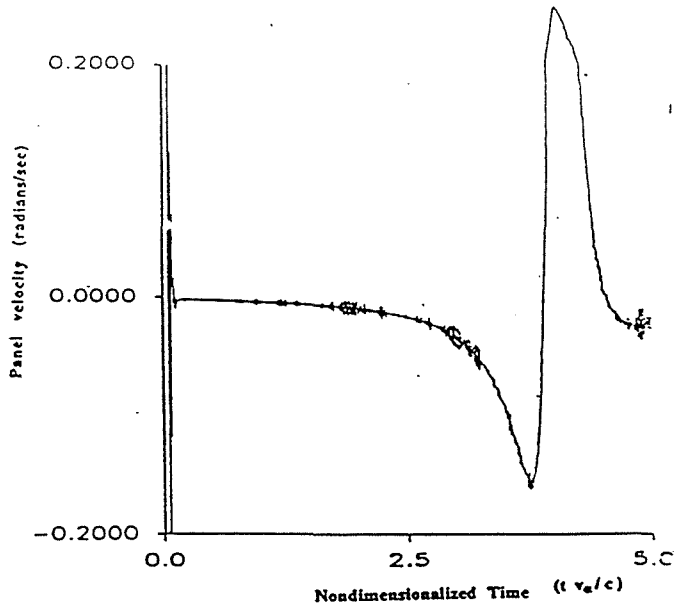

Figure 4. Panel angular velocities at the leading and trailing edges using the controller designed based on quadratic performance index

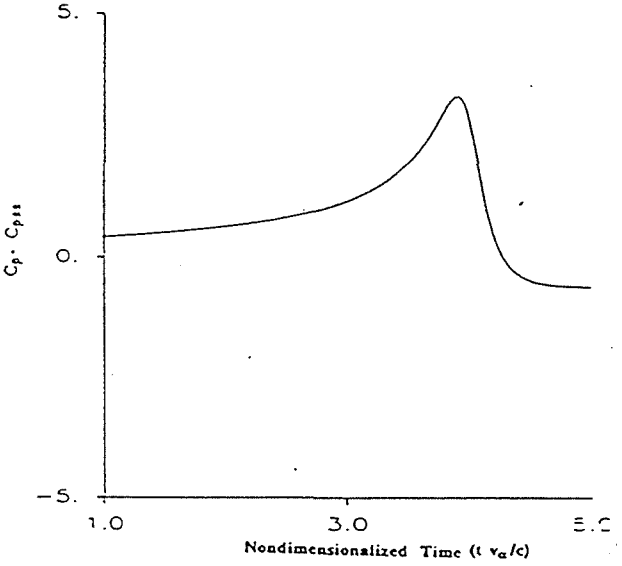

Figure 5. Variation of $C_p - C_{pss}$ with time

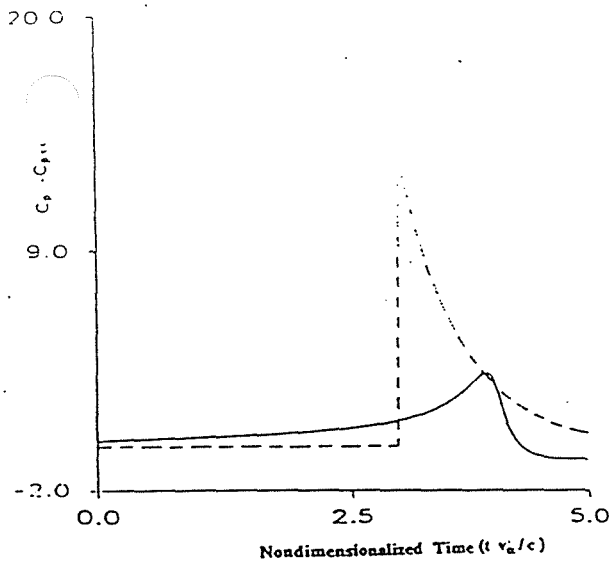

Figure 6. Constructed Cp - Cpss variation

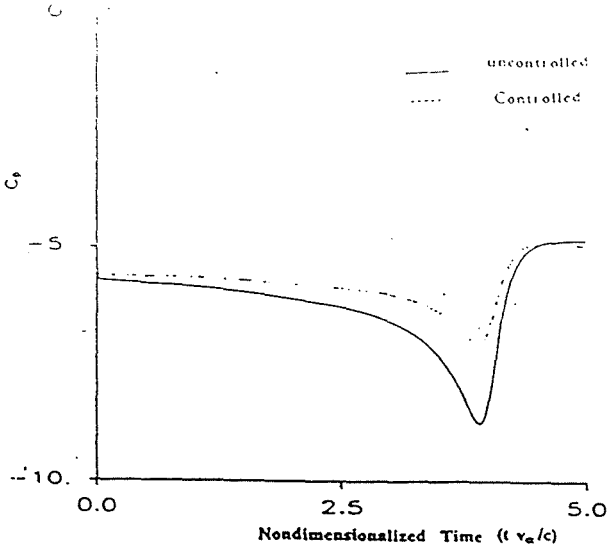

Figure 9. Variation of coefficient of pressure using a H-infinity controller

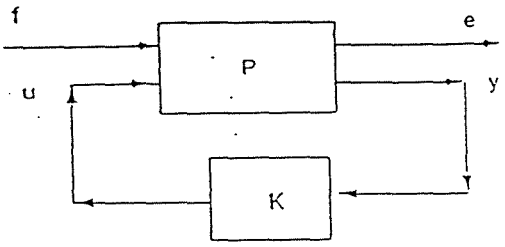

Figure 7. Block diagram for the H-infinity controller

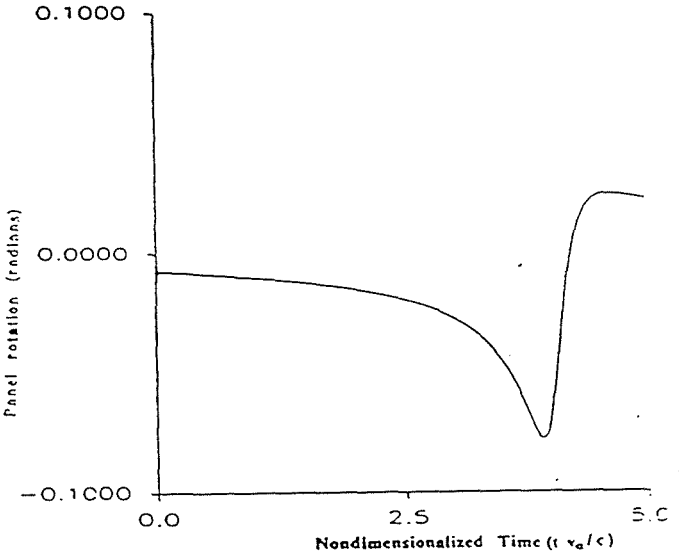

Figure 10. Panel angular rotations at the leading and trailing edges using the H-infinity controller

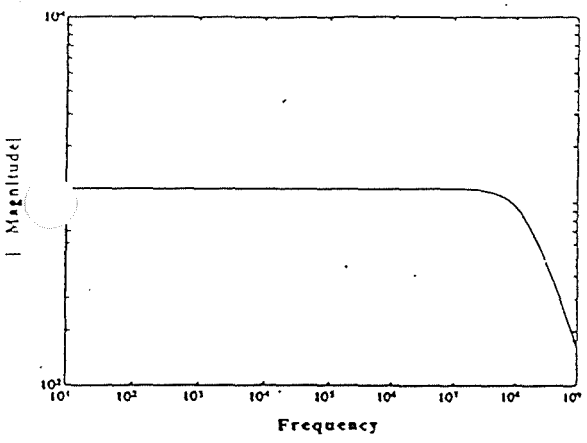

Figure 8. Bode plot for the H-infinity controller